# On the Energy Efficiency-Spectral Efficiency Trade-off over the MIMO Rayleigh Fading Channel

Fabien Héliot, *Member, IEEE,* Muhammad Ali Imran, *Member, IEEE,* and Rahim Tafazolli, *Senior Member, IEEE*

***Abstract*—Along with spectral efficiency (SE), energy efficiency (EE) is becoming one of the key performance evaluation criteria for communication system. These two criteria, which are conflicting, can be linked through their trade-off. The EE-SE trade-off for the multi-input multi-output (MIMO) Rayleigh fading channel has been accurately approximated in the past but only in the low-SE regime. In this paper, we propose a novel and more generic closed-form approximation of this trade-off which exhibits a greater accuracy for a wider range of SE values and antenna configurations. Our expression has been here utilized for assessing analytically the EE gain of MIMO over single-input single-output (SISO) system for two different types of power consumption models (PCMs): the theoretical PCM, where only the transmit power is considered as consumed power; and a more realistic PCM accounting for the fixed consumed power and amplifier inefficiency. Our analysis unfolds the large mismatch between theoretical and practical MIMO vs. SISO EE gains; the EE gain increases both with the SE and the number of antennas in theory, which indicates that MIMO is a promising EE enabler; whereas it remains small and decreases with the number of transmit antennas when a realistic PCM is considered.**

***Index Terms*—Energy efficiency, Spectral efficiency, Trade-off, MIMO, Rayleigh channels.**

## I. Introduction

Energy efficiency (EE) can be seen as a mature field of research in communication, at least for power-limited applications such as battery-driven system [1], e.g. mobile terminal, underwater acoustic telemetry [2], or wireless ad-hoc and sensor networks [3], [4]. However, in the current context of increasing energy demand and price, it can be considered as a new frontier for communication network. Indeed, network operators are currently driving the research agenda towards more energy efficient network as a whole in order to decrease their ever-growing operational costs. The first signs of this trend can already be seen in the development of future mobile systems such as long term evolution-advanced (LTE-A) [5].

The efficiency of a communication system has traditionally been measured in terms of spectral efficiency (SE), which is directly related to the channel capacity in bit/s. This metric indicates how efficiently a limited frequency spectrum is utilized, however, it fails to provide any insight on how efficiently the energy is consumed. Such an insight can be given by incorporating an EE metric in the performance evaluation framework. Various EE metrics have been defined in the literature; apart from the widely used energy-per-bit to noise power spectral density ratio [2], [6]–[8], i.e. $E_b/N_0$, one can also use the bit-per-Joule capacity [2], [9], the rate per energy [10] or the Joule-per-bit [3] as an EE metric.

The EE of a communication system is closely related to its power consumption and the main power-hungry component of a traditional cellular network is the base station (BS). In most of the theoretical studies [2], [6]–[8], the total consumed power of a transmitting node such as a BS has been assumed to be equal to its transmit power, whereas in reality, it accounts for various power elements such as cooling, processing or amplifying power. Thus, in order to get a full picture of the total consumed power in a system and evaluate fairly its EE, a more realistic power consumption model (PCM) must be defined for each node, such as the ones recently proposed in [11]–[13] for the BS of various communication systems, e.g. GSM, UMTS and LTE. The PCMs in [11] and [12] are linear, whereas the one in [13] is nearly-linear.

Minimizing the consumed energy, or equivalently maximizing the EE, while maximizing the SE are conflicting objectives and, consequently, they can be linked together through their trade-off. The concept of EE-SE trade-off has first been introduced in [6], where an approximation of this trade-off has been derived for the white and colored noises, as well as multi-input multi-output (MIMO) fading channels based on the first and second derivatives of the channel capacity. This linear approximation is accurate in the low-SE regime but largely inaccurate otherwise. This work has inspired numerous other works where the same analytical method was used to approximate the EE-SE trade-off of correlated multi antenna [7], multi-user [14], multi-hop [3], [8], or cooperative [15]–[17] communication system in the low-SE regime. In general, the problem of defining a closed-form expression for the EE-SE trade-off is equivalent to obtaining an explicit expression for the inverse function of the channel capacity per unit bandwidth. This has so far been proved feasible only for the additive white Gaussian noise (AWGN) channel and deterministic channel with colored noise in [2] and [6], respectively, and it explains why the various works previously cited have resorted to approximation instead of explicit expression.

In this paper, we derive a novel and generic closed-form approximation (CFA) of the EE-SE trade-off over the MIMO Rayleigh fading channel and demonstrate its accuracy for numerous antenna configurations and a wider range of SE values than the approximation in [6]. In Section II, we first introduce the EE-SE trade-off concept and detail the two main approaches that have been followed in the past for deriving explicit expression of this trade-off when assuming a

Paper approved by N. C. Beaulieu, the Editor for Wireless Communication Theory of the IEEE Communications Society. Manuscript received April 11, 2011; revised October 11, 2011; accepted December 24, 2011.

The authors are with the Centre for Communication Systems Research, Faculty of Electronics & Physical Sciences, University of Surrey, Guildford GU2 7XH, UK (e-mail: F.Heliot@Surrey.ac.uk).

The research leading to these results has received funding from the European Commission's Seventh Framework Programme FP7/2007-2013 under grant agreement n°247733-project EARTH.

theoretical PCM. We then briefly introduce our new approach based on CFA and show how to extend the formulation of the EE-SE trade-off for linear and double linear PCMs such as the ones defined in [11]–[13]. In Section III, we recall the classic point-to-point MIMO system model and introduce the two prevailing methods that can be utilized for explicitly formulating the ergodic MIMO channel capacity. In Section IV, we then demonstrate how to obtain an accurate CFA of the EE-SE trade-off by using one of these methods and provide a formal proof of the derivation for the symmetric antenna configuration, i.e. when transmit and receive nodes have the same number of antennas. Next, we extend our derivation for any antenna configuration by designing a simple parametric function through the use of a heuristic curve fitting method [18], [19]. Numerical results show the accuracy of our approximation for a wide range of SE values and numerous antenna configurations. In Section V, we derive the theoretical and practical EE gain limits of MIMO over single-input single-output (SISO) system in the low and high-SE regimes by using the explicit formulation of the EE-SE trade-off for the multiple-input single-output (MISO) channel and the simplified expression of our CFA for the MIMO channel, which can be found in the Appendix. Conclusions are finally drawn in Section VI. Some preliminary works have been carried out in [20] and [21] regarding the derivation of the EE-SE trade-off CFA for MIMO and EE analysis of MIMO system, respectively. Herein, our CFA of the EE-SE trade-off has been simplified as well as made more generic and a formal proof of its derivation has been given. Furthermore, a more detailed analysis of the MIMO/SISO EE gain has been conducted based on our refined CFA and a more realistic double linear PCM for assessing the real potential of MIMO in terms of EE over the Rayleigh fading channel.

## II. EE-SE Trade-off Concept and Related Works

### A. EE-SE Trade-off Concept

In simple words, the concept of EE-SE trade-off can be described as how to express EE as a function of SE. Let $R$ (bit/s) be the achievable rate of an encoder and $P_\Sigma$ (Watt) be the total consumed power for transmitting data at this rate, then the EE can either be expressed in terms of energy-per-bit, $E_b$, or bit-per-Joule capacity, $C_J$, as $E_b = P_\Sigma/R$ or $C_J = R/P_\Sigma$, respectively. Note that $P_\Sigma = P$ in most of the theoretical works related to the EE-SE trade-off [2], [6]–[8], where $P$ (Watt) is the transmit power. As far as the maximum achievable SE or equivalently the channel capacity per unit bandwidth $C$ (bit/s/Hz) is concerned, it can be expressed as

$$C = f(\gamma) \tag{1}$$

via the Shannon's capacity theorem [22], where $\gamma = P/(N_0 W)$ is the signal-to-noise ratio (SNR), $W$ (Hz) is the bandwidth and $N_0$ (Joule) is the noise spectral density. In addition, $f(\gamma) = \log_2(1+\gamma)$ in the AWGN channel case and without loss of generality $f : \gamma \in [0, +\infty) \mapsto C \in [0, +\infty)$. Let $S = R/W$ (bit/s/Hz) be the achievable SE, then $\gamma$ can be re-expressed as a function of both the SE and EE such that

$$\gamma = \frac{P}{N_0 W} = \frac{S E_b}{N_0}. \tag{2}$$

Inserting (2) into (1), the EE-SE trade-off is simply expressed as follows

$$\frac{E_b}{N_0} = \frac{f^{-1}(C)}{S}, \tag{3}$$

where $f^{-1} : C \in [0, +\infty) \mapsto \gamma \in [0, +\infty)$ is the inverse function of $f$. Equation (3) indicates that a straightforward solution for finding an explicit expression of the EE-SE trade-off boils down to obtaining an explicit expression for $f^{-1}(C)$. For instance in the AWGN channel case $C = f(\gamma) = \log_2(1+\gamma)$ and, hence, $f^{-1}(C)$ is directly given by $\gamma = f^{-1}(C) = 2^C - 1$ [2], [6]. However, in cases where $f(\gamma)$ does not have a straightforward formulation, e.g. MIMO Rayleigh fading channel, approximating $f^{-1}(C)$ can provide an acceptable solution. In [6], it has been stated that the EE of a communication system depends mainly on its SE in the low-power/low-SE regime such that the EE-SE trade-off can be approximated as (equation (28) of [6])

$$\frac{E_b}{N_0} \gtrsim \frac{E_b}{N_{0\,\min}} 2^{\frac{C}{S_0}}, \tag{4}$$

where $\frac{E_b}{N_{0\,\min}} = \frac{\ln(2)}{\dot{f}(0)}$ and $S_0 = \frac{2[\dot{f}(0)]^2}{-\ddot{f}(0)}$ are the minimum energy-per-bit and the slope of the SE, respectively, and $\dot{f}(0)$ and $\ddot{f}(0)$ are the first and second order derivatives of $f(\gamma)$ when $\gamma = 0$. This method is in effect quite generic and, thus, it can be used to approximate the EE-SE trade-off of any communication channels or systems for which an explicit expression of its maximum achievable SE as a function of $\gamma$, i.e. $f(\gamma)$, exists and is twice differentiable. It has first been utilized in [6] for approximating the EE-SE trade-off over the AWGN and various fading channels, such as the MIMO Rayleigh and Rician channels. Because of its simplicity, this approach has gained popularity and it has been extended over the years to most of the communication scenarios of interest, as we previously mentioned in the introduction. However, the main shortcoming of this approach is its rather limited range of SE values for which it is accurate. Indeed, it is by design limited to the low-SE regime and, thus, it cannot be used for assessing the EE of future communication system such as LTE which are meant to operate in the mid-high SE region.

So far, the two main approaches for obtaining explicit expression of the EE-SE trade-off have been either to use the explicit expression of $f(\gamma)$ for finding an explicit solution to $f^{-1}(C)$ or to use the explicit expression of $f(\gamma)$ for approximating $f^{-1}(C)$. Another approach would be to use an accurate CFA of $f(\gamma)$, i.e. $f(\gamma) \approx \tilde{f}(\gamma)$ for finding an explicit solution to $f^{-1}(C)$, as it is here presented for the MIMO Rayleigh fading scenario. Note that we have recently used the same approach for accurately and explicitly expressing the EE-SE trade-off in the uplink of cellular system [23].

### B. EE-SE Trade-off for Realistic PCMs

In a practical setting, $P$ is not equal to $P_\Sigma$. For instance in [11] and [12], $P_\Sigma$ is expressed as

$$P_\Sigma = N_{\text{Sector}} N_{\text{PApSec}} (P_{\text{Tx}}/\mu_{\text{PA}} + P_{\text{SP}})(1 + C_{\text{C}})(1 + C_{\text{PSBB}}), \tag{5}$$

where $N_{\text{Sector}}$ is the number of sector, $N_{\text{PApSec}}$ is the number of power amplifier (PA) per sector, $P_{\text{Tx}}$ is the transmit power

per PA, $\mu_{\text{PA}}$ is the PA efficiency, $P_{\text{SP}}$ is the signal processing overhead, $C_{\text{C}}$ is the cooling loss and $C_{\text{PSBB}}$ is the battery backup and power supply loss. In general, the number of PAs of a BS is equal to the number of transmit antennas such that $N_{\text{Sector}}N_{\text{PApSec}} = t$, and the linear PCM of (5) is equivalent to $P_\Sigma = t(\Delta_P P_{\text{Tx}} + \overline{P}_0)$, where $\Delta_P = (1+C_{\text{C}})(1+C_{\text{PSBB}})/\mu_{\text{PA}}$ and $\overline{P}_0 = P_{\text{SP}}(1+C_{\text{C}})(1+C_{\text{PSBB}})$ are the slope and constant part of the PCM, respectively. This BS PCM has been refined in [13] such that the power consumption of extra BS components, e.g. direct current (DC)-DC and analog current (AC)-DC converters, have also been included. Even though this model takes into account the non-linearity of the PA, it has been shown in [13] that the relation between relative radio frequency (RF) output power and BS power consumption is nearly-linear and, consequently, a linear abstraction of this model has been defined for the 2x2 antenna setting and different types of BS in Table 7 of [13]. Moreover, as it is explained in [13], it is anticipated that the power consumption of components like DC-DC/AC-DC converter and cooling unit will not grow linearly with the number of antennas and, thus, the PCM in (5) gives an upper bound on the power consumption of a BS with $t$ transmit antennas. A more realistic double linear PCM, i.e. linear both in terms of $P$ and $t$, would consider that only one part of the overhead power grows linearly with $t$ and one part remains fixed such that

$$P_\Sigma = t(\Delta_P P_{\text{Tx}} + P_0) + P_1, \tag{6}$$

which is consistent with the BS PCM recently proposed in [24]. Substituting $P$ in (2) by $P_\Sigma$ in (6), we can generalize the EE-SE trade-off in (3) as follows

$$\frac{E_b}{N_0} = \frac{1}{S}\left[\Delta_P f^{-1}(C) + \frac{tP_0 + P_1}{N}\right], \tag{7}$$

where $N = N_0 W$ is the noise power. Note that (7) reverts to (3) when $\Delta_P = 1$ and $P_0 = P_1 = 0$, i.e. in the theoretical case.

## III. Ergodic Capacity of MIMO Rayleigh Fading Channel: Explicit Expression vs. CFA

Let us consider a classic MIMO communication system where a signal $\mathbf{x} \in \mathbb{C}^{t\times 1}$ is transmitted over $t$ transmit antennas and is received by $r$ receive antennas as

$$\mathbf{y} = \mathbf{H}\mathbf{x} + \mathbf{n}, \tag{8}$$

where $\mathbf{H} \in \mathbb{C}^{r\times t}$ and $\mathbf{n} \in \mathbb{C}^{r\times 1}$ characterize the MIMO channel and the AWGN noise, respectively. Let $\mathbf{H}$ be a random matrix having independent and identically distributed (i.i.d.) complex circular Gaussian entries with zero-mean and unit variance, and let $\mathbf{n}$ belongs to an $r$-dimensional complex zero-mean circular symmetric Gaussian distribution with variance $N$ per dimension, i.e. $\mathbf{n} \sim \mathcal{N}_c(\mathbf{0}_r, N\mathbf{I}_r)$, where $\mathbf{0}_r$ and $\mathbf{I}_r$ denote the all-zero matrix and the identity matrix, respectively, of dimension $r \times r$. In addition, let $\mathbf{x} \sim \mathcal{N}_c(\mathbf{0}_t, (P/t)\mathbf{I}_t)$, where $\text{tr}(\text{E}\left\{\mathbf{x}\mathbf{x}^\dagger\right\}) = P$, $\text{tr}(.)$ and $\text{E}\{.\}$ stand for the trace and expectation, respectively. The ergodic channel capacity per unit bandwidth of the MIMO Rayleigh fading channel is accordingly expressed as [25]

$$C = f(\gamma) \triangleq \text{E}_{\mathbf{H}}\left\{\log_2\left|\mathbf{I}_r + \frac{\gamma}{t}\mathbf{H}\mathbf{H}^\dagger\right|\right\}, \tag{9}$$

where $|.|$ is the determinant of a matrix. In the literature, two main approaches have been used for deriving either closed-form expressions or approximations of the ergodic capacity as in (9). In [25], the expression of $C$ has been simplified into an analytical formula by computing the expectation of the ordered eigenvalues of the Wishart matrix $\mathcal{W} \triangleq \mathbf{H}\mathbf{H}^\dagger$ or $\mathbf{H}^\dagger\mathbf{H}$ if $r < t$ or $r \geq t$, respectively. This work has sparkled a flurry of interest in finding proper closed-form expressions of the ergodic capacity [26]–[29]. Even though these expressions are perfectly accurate, their formulations are cumbersome. For instance, $f(\gamma)$ is given by

$$\begin{aligned} f(\gamma) \;=& \sum_{k=0}^{m-1}\frac{k!}{(k+d)!}\sum_{l_1=0}^{k}\sum_{l_2=0}^{k}(-1)^{l_1+l_2}A_{l_1}(k,d)A_{l_2}(k,d) \\ &\times \widehat{C}_{l_1+l_2+d}\left(\frac{t}{\gamma}\right) \end{aligned} \tag{10}$$

in [26], where $d \triangleq n-m$, $n \triangleq \max(t,r)$, $m \triangleq \min(t,r)$ and $A_l(k,d) \triangleq \frac{(k+d)!}{(k-l)!(d+l)!l!}$. In addition,

$$\begin{aligned} \widehat{C}_i(x) \triangleq& \frac{1}{\ln(2)}\sum_{j=0}^{i}\frac{i!}{(i-j)!}\left[(-x)^{i-j}e^x E_1(x) + \sum_{k=1}^{i-j}(k-1)!\right. \\ &\left.\times(-x)^{i-j-k}\right], \end{aligned} \tag{11}$$

where $E_1(x) = \int_x^\infty \frac{e^{-t}}{t}dt$ is the exponential integral function. In the case that $t = r = 1$, equation (10) simplifies as $f(\gamma) = e^{1/\gamma}E_1(1/\gamma)$, which already does not have an explicit formulation for $f^{-1}(C)$. In Parallel to these works, a CFA of (9) has been derived in [30] by relying on asymptotical analysis and random matrix theory. This approach yields an approximation of the capacity, i.e. $C \approx \widetilde{f}(\gamma)$, which is obviously less accurate than the former approach, but has the advantage of being expressed in a simple form [30]

$$\begin{aligned} \widetilde{f}(\gamma) \;=& -\frac{t}{\ln(2)}\left[-(1+\beta)\ln(\sqrt{\gamma}) + q_0(\gamma)r_0(\gamma) + \ln(r_0(\gamma))\right. \\ &\left.+\beta\ln\left(\frac{q_0(\gamma)}{\beta}\right)\right], \end{aligned} \tag{12}$$

where

$$\begin{aligned} q_0(\gamma) \;&=\; \frac{-1-u(\gamma)+v(\gamma)}{2\sqrt{\gamma}} \\ r_0(\gamma) \;&=\; \frac{-1+u(\gamma)+v(\gamma)}{2\sqrt{\gamma}} \end{aligned}, \tag{13}$$

$u(\gamma) = \gamma(1-\beta)$, $v(\gamma) = \sqrt{1+2\gamma(1+\beta)+\gamma^2(1-\beta)^2}$ and $\beta \triangleq r/t$. Moreover, it can be demonstrated (see Section A of the Appendix) that $\widetilde{f}(\gamma)$ in (12) can be transformed as

$$\begin{aligned} \widetilde{f}(\gamma) =& \frac{1}{\ln(2)}\underbrace{\left[t\left(-c+[1+\overline{q}_0(\gamma)]^{-1}+\ln[1+\overline{q}_0(\gamma)]\right)\right]}_{S_t} \\ &+\frac{1}{\ln(2)}\underbrace{\left[r\left(-c+[1+\overline{r}_0(\gamma)]^{-1}+\ln[1+\overline{r}_0(\gamma)]\right)\right]}_{S_r}, \end{aligned} \tag{14}$$

where $\overline{q}_0(\gamma) \triangleq 2\sqrt{\gamma}q_0(\gamma)+1$, $\overline{r}_0(\gamma) \triangleq 2\sqrt{\gamma}r_0(\gamma)+1$, and $c = \frac{1}{2}+\ln(2)$. This accurate approximation has been derived

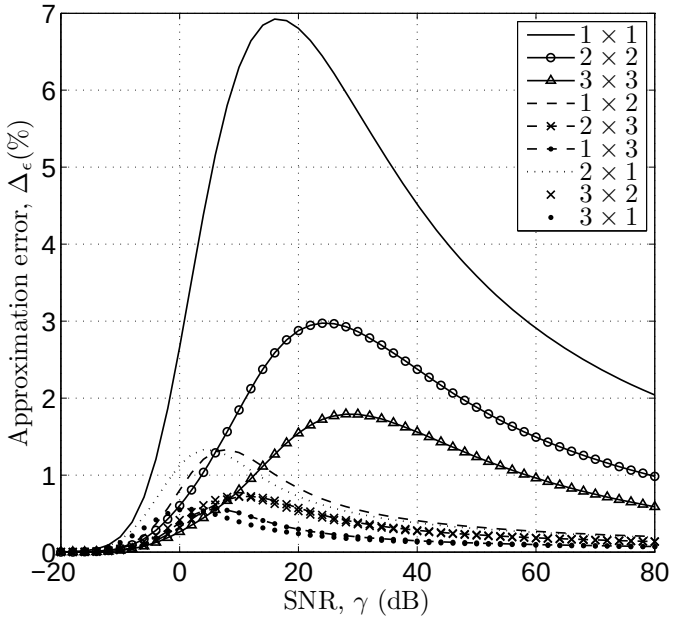


Fig. 1. Approximation error in % between $\widetilde{f}(\gamma)$ in (12) and $f(\gamma)$ in (10) as a function of $\gamma$ (dB) for various $r\times t$ antenna configurations.

by assuming a large number of antennas $t$ and $r$, however, its accuracy has been deemed acceptable even for a small number of antennas in [30]. In order to illustrate the accuracy of this approximation, we plot in Fig. 1 $\Delta_\epsilon \triangleq 100|f(\gamma)-\widetilde{f}(\gamma)|/|f(\gamma)|$ vs. $\gamma$ (dB) for various $t$ and $r$ values, where $\Delta_\epsilon$ denotes the approximation error in percentage between $f(\gamma)$ in (10) and $\widetilde{f}(\gamma)$ in (12). The results first show that the accuracy of $\widetilde{f}(\gamma)$ increases with the number of antennas. In the asymmetric scenario, i.e. $r\neq t$, the accuracy is already acceptable for the $r=1\times t=2$ and $r=2\times t=1$ antenna configurations. In this case, the maximum of $\Delta_\epsilon$ is around 1.3%, whereas the average $\Delta_\epsilon$ is around 0.5%. It can also be noticed that the accuracy increases as the antenna configuration becomes more asymmetric. In the symmetric scenario, i.e. $t=r$, more antennas are required for reaching an acceptable accuracy such that the maximum of $\Delta_\epsilon$ is around 1.8% and the average $\Delta_\epsilon$ is below 1% when $t=r=3$.

## IV. Closed-form Approximation of the EE-SE Trade-off for MIMO Systems

Despite being less accurate than $f(\gamma)$, the main advantage of $\widetilde{f}(\gamma)$ over $f(\gamma)$ is the fact that the inverse function of $\widetilde{f}(\gamma)$, i.e. $\widetilde{f}^{-1}(C)$, can be expressed into a closed-form. Consequently, an accurate CFA of the EE-SE trade-off can be formulated as

$$\gamma\approx\widetilde{f}^{-1}(C) = \frac{1}{2(1+\beta)}\left\{-1+\left(1+\left[W_0\left(g_t(C)\right)\right]^{-1}\right)\times\left(1+\left[W_0\left(g_r(C)\right)\right]^{-1}\right)\right\} \tag{15}$$

in the MIMO Rayleigh fading case, where $W_0(x)$ denotes the real branch of the Lambert function [31]. The Lambert $W$ function is the inverse function of $f(w)=we^w$ and, thus, it satisfies $W(z)e^{W(z)}=z$, with $w,z\in\mathbb{C}$ [31]. Its real branch, $W_0$, is such that $W_0:\mathcal{D}_{W_0}=[-e^{-1},+\infty)\mapsto[-1,+\infty)$ and is monotonically increasing over $\mathcal{D}_{W_0}$. Moreover, the functions $g_t(x)$ and $g_r(x)$ in (15) are defined as

$$\begin{aligned} g_t(x)&\triangleq -2^{-\left(\frac{x+h(x)}{2t}+1\right)}e^{-\frac{1}{2}} \text{ and}\\ g_r(x)&\triangleq -2^{-\left(\frac{x-h(x)}{2r}+1\right)}e^{-\frac{1}{2}}, \end{aligned} \tag{16}$$

respectively, and the function $h(x)$ in (16) is expressed as

$$h(x)\triangleq\zeta m\log_2\left(1-\eta_0\left[1-\cosh\left(\frac{x\ln(2)}{m[\eta(\overline{\beta})+\log_2(\eta_0)]}\right)^{\eta_1}\right]\right), \tag{17}$$

with $\zeta\triangleq\text{sgn}(\ln(\beta))$ and sgn$(x)\triangleq-1$, 0 or 1 if $x<0$, $x=0$ or $x>0$ such that $h(x)=0$ when $\beta=1$. In addition, $\eta(\overline{\beta})=\frac{1}{\ln(2)}\left[-1+2\overline{\beta}\ln\left(\frac{\overline{\beta}}{\overline{\beta}-1}\right)\right]$ in (17), where $\overline{\beta}\triangleq n/m$, $\overline{\beta}\in[1,+\infty)$, and the values of the parameters $\eta_0$ and $\eta_1$ are

$$\eta_0=\begin{cases}1 & ,\text{if } \overline{\beta}\in[2,+\infty)\\ \text{see Table I} & ,\text{if } \overline{\beta}\in(1,2)\end{cases} \text{ and}$$
$$\eta_1=\begin{cases}\eta(\overline{\beta}) & ,\text{if } \overline{\beta}\in[2,+\infty)\\ \text{see Table I} & ,\text{if } \overline{\beta}\in(1,2)\end{cases}.$$

Since $\zeta=0$ when $\beta=1$, it implies that $g_t(x)=g_r(x)$ and, thus, our CFA in (15) simplifies as

$$\widetilde{f}^{-1}(C)=\frac{1}{4}\left\{-1+\left(1+\left[W_0\left(-2^{-\left(\frac{C}{2r}+1\right)}e^{-\frac{1}{2}}\right)\right]^{-1}\right)^2\right\} \tag{18}$$

in the symmetric antenna configuration, i.e. when $t=r$.

### A. Case of $t=r$

*Proof:* Let $S_t=t\left(-c+[1+\overline{q}_0(\gamma)]^{-1}+\ln[1+\overline{q}_0(\gamma)]\right)$ in (14), it is equivalent to $-(S_t/t+c)=-[1+\overline{q}_0(\gamma)]^{-1}+\ln\left([1+\overline{q}_0(\gamma)]^{-1}\right)$ as well as

$$-e^{-(S_t/t+c)}=-[1+\overline{q}_0(\gamma)]^{-1}e^{-[1+\overline{q}_0(\gamma)]^{-1}}. \tag{19}$$

Knowing that $S_t\in\mathbb{R}^+$ and $c=\frac{1}{2}+\ln(2)>1$, it implies that $-e^{-(S_t/t+c)}\in\left[-\frac{1}{2}e^{-\frac{1}{2}},0\right]$ belongs to the domain of $W_0$, i.e. $\mathcal{D}_{W_0}$. Consequently, we can reformulate (19) as

$$\begin{aligned} -[1+\overline{q}_0(\gamma)]^{-1} &= W_0\left(-e^{-(S_t/t+c)}\right),\\ \overline{q}_0(\gamma) &= -\left(1+\left[W_0\left(-e^{-(S_t/t+c)}\right)\right]^{-1}\right). \end{aligned} \tag{20}$$

Following the same reasoning, it can also be proved that

$$\overline{r}_0(\gamma)=-\left(1+\left[W_0\left(-e^{-(S_r/r+c)}\right)\right]^{-1}\right). \tag{21}$$

In addition, $\overline{q}_0(\gamma)\overline{r}_0(\gamma) = -u(\gamma)^2+v(\gamma)^2$ which further simplifies as

$$\overline{q}_0(\gamma)\overline{r}_0(\gamma)=1+2\gamma(1+\beta) \tag{22}$$

by using the definitions of $u(\gamma)$ and $v(\gamma)$ given below (13). We then obtain that

$$\gamma = \frac{1}{2(1+\beta)}\left\{-1+\left(1+\left[W_0\left(-e^{-(S_t/t+c)}\right)\right]^{-1}\right)\times\left(1+\left[W_0\left(-e^{-(S_r/r+c)}\right)\right]^{-1}\right)\right\} \tag{23}$$

TABLE I
PARAMETERS $\eta_0$ AND $\eta_1$ VALUES AS A FUNCTION OF $\overline{\beta}$, FOR VARIOUS $\overline{\beta} \in (1,2)$

| $\overline{\beta}$ | 10/9 | 9/8 | 8/7 | 7/6 | 6/5 | 5/4 | 9/7 | 4/3 | 7/5 | 10/7 | 3/2 | 8/5 | 5/3 | 7/4 | 9/5 |
|---|---|---|---|---|---|---|---|---|---|---|---|---|---|---|---|
| $\eta_0$ | 0.377 | 0.373 | 0.366 | 0.365 | 0.369 | 0.384 | 0.508 | 0.4285 | 0.528 | 0.608 | 0.1315 | 0.1621 | 0.1808 | 0.2028 | 0.2153 |
| $\eta_1$ | 3.914 | 3.835 | 3.705 | 3.515 | 3.266 | 2.968 | 3.059 | $\varphi = \log_2(\eta_0) + \eta(\overline{\beta})$ | 2.682 | 2.751 | $\varphi$ | $\varphi$ | $\varphi$ | $\varphi$ | $\varphi$ |

by inserting (20) and (21) in (22). Finally, when $t = r$ then $\beta = 1$ and, hence, $q_0(\gamma) = r_0(\gamma)$ in (13). Therefore, $S_t = S_r$ and $C = f(\gamma) \approx \widetilde{f}(\gamma) = 2S_t/\ln(2)$ in (14) which in turn implies that

$$S_t = S_r \approx C\ln(2)/2. \tag{24}$$

Inserting (24) in (23), we finally obtain (18). ■

### B. Case of $t \neq r$

According to (23), the problem of finding an explicit formulation for the EE-SE trade-off as given in (15) boils down to expressing both $S_t$ and $S_r$ as a function of $C$ in (23). Indeed, $C \approx \widetilde{f}(\gamma) = (S_r + S_t)/\ln(2)$ according to (14) and, thus, if $S_r - S_t$ could be formulated as a function of $C$, then, it would become easy to express $S_t$ and $S_r$ as a function of $C$ by solving a simple system of linear equations. In the following, we propose an accurate approximation of $S_r - S_t$ as a function of $C$ by means of a parametric function $\phi_{t,r}(C)$ which is defined as follows

$$\phi_{t,r}(C) \approx e^{\frac{S_r - S_t}{m}}, \tag{25}$$

where $S_r - S_t = \ln(2^t[1 + \overline{r}_0(\gamma)]^r) - \ln(2^r[1 + \overline{q}_0(\gamma)]^t)$ (see Section B of the Appendix).

In the heuristic curve fitting method proposed in [18], a parametric function is designed in terms of elementary functions and three independent parameters for solving a curve fitting problem. In this paper, we use this method to design the parametric function $\phi_{t,r}(C)$ that tightly fits $e^{\frac{S_r - S_t}{m}}$ for $\beta < 1$. We first numerically evaluated $e^{\frac{S_r - S_t}{m}}$ as a function of $C/m$ for different values of $\beta$ and then collected the resulting curves in Fig. 2. It can be noticed that $e^{\frac{S_r - S_t}{m}}$ presents the feature of an exponential function at low $C$ and of a linear function at high $C$ (in logarithmic scale). In addition, this function is monotonic and its value at $C = 0$ is 1. In order to define the function that best fits the curves of Fig. 2, the curve fitting method lead us to the following parametric function

$$\phi_{t,r}(C/m) = 1 + \eta_0 \left[ \cosh\left\{ \frac{(C/m)\ln(2)}{\eta(\overline{\beta}) + \log_2(\eta_0)} \right\}^{\eta_1} - 1 \right], \tag{26}$$

which provides a satisfying approximation as it is illustrated in Fig. 2, i.e. the average approximation errors (as defined in Section III) are 0.75, 0.24, 0.14, 0.59, 0.26, 0.54, 0.65% for $\beta = \{4/5, 2/3, 5/9, 1/2, 1/3, 1/10\}$, $\eta_0 = \{0.384, 0.1315, 0.2153, 1, 1, 1\}$, and $\eta_1 = \{2.968, \eta(3/2) + \log 2(0.1315), \eta(9/5) + \log 2(0.2153), \eta(2), \eta(3), \eta(10)\}$, respectively. The parametric function in (24) has been defined for the case of $\beta < 1$, however, it can simply be extended to the case of $\beta > 1$ as $\phi_{t,r}(C/m) = \phi_{t,r}(C/m)^{-1}$ such that

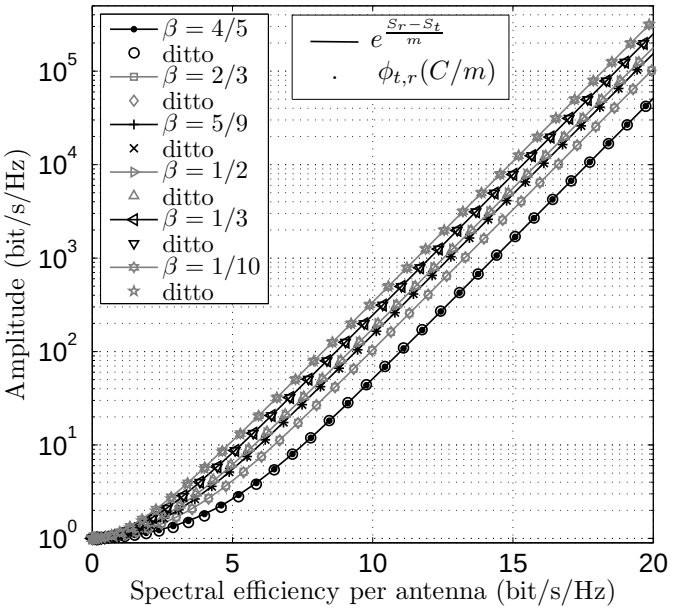


Fig. 2. Comparison of $e^{\frac{S_r - S_t}{m}}$ with our parametric function $\phi_{t,r}(C/m)$ as a function of the SE per antenna for various receive/transmit antenna ratios.

$$\phi_{t,r}(C) = \left( 1 + \eta_0 \left[ \cosh\left\{ \frac{C\ln(2)}{m[\eta(\overline{\beta}) + \log_2(\eta_0)]} \right\}^{\eta_1} - 1 \right] \right)^{-\zeta}, \tag{27}$$

for $\beta \in (0,1) \cup (1, +\infty)$ or equivalently $\overline{\beta} \in (1, +\infty)$, where the values of the parameters $\eta_0$ and $\eta_1$ are the same for $\beta = x$ and $\beta = 1/x$ and, thus, can be expressed as a function of $\overline{\beta}$. Inserting (27) in (25), we can re-express the difference between $S_r$ and $S_t$ as $S_r - S_t \approx -\ln(2)h(C)$, where $h(x)$ is given in (17). Moreover, since $S_r + S_t \approx C\ln(2)$, $S_t$ and $S_r$ can be approximated as a function of $C$ as follows

$$\begin{aligned} S_t(C) &\approx \ln(2)[C + h(C)]/2, \text{ and} \\ S_r(C) &\approx \ln(2)[C - h(C)]/2. \end{aligned} \tag{28}$$

Our CFA of the EE-SE trade-off in (15) has finally been obtained by inserting (28) in (23).

Notice that in the case of $\overline{\beta} \in (1,2)$, the tightness of $\phi_{t,r}(C)$ can be adjusted in (27) via the parameters $\eta_0$ and $\eta_1$ such that the following mean squared error equation is minimized

$$\frac{1}{10N+1} \sum_{C=0}^{N} |(S_r(C) - S_t(C)) - (-\ln(2)h(C))|^2 \leq \varepsilon_0. \tag{29}$$

Using (29), we have obtained the coefficients $\eta_0$ and $\eta_1$, which are collected in Table I, for $N = 40$, $\varepsilon_0 = 2 \times 10^{-3}$ and with an incremental step of 0.1 bit/s/Hz for $C$.

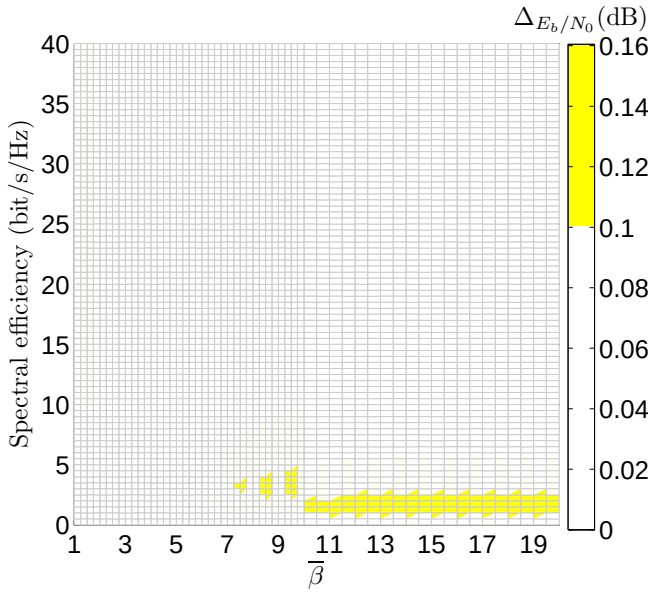


Fig. 3. Approximation error in terms of $E_b/N_0$ (dB) between the nearly-exact $E_b/N_0$ and our CFAs in (15) and (18) as a function of the SE and $\overline{\beta} = \max\{t,r\}/\min\{t,r\}$.

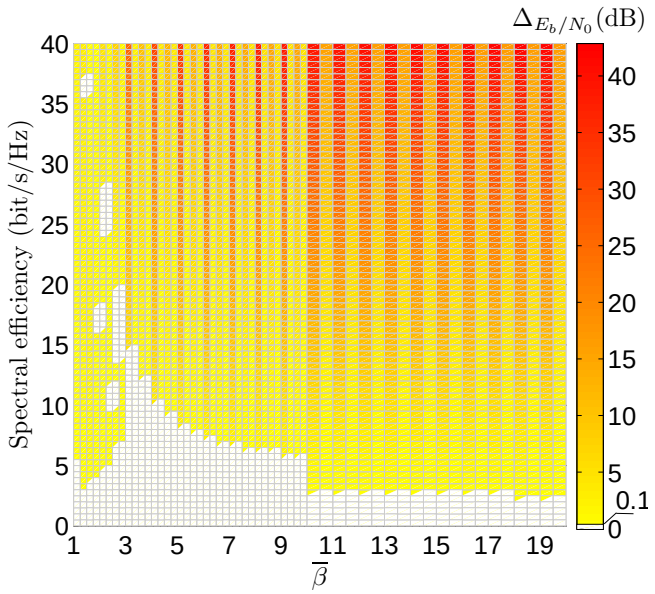


Fig. 4. Approximation error in terms of $E_b/N_0$ (dB) between the nearly-exact $E_b/N_0$ and the approximation method of [6] as a function of the SE and $\overline{\beta} = \max\{t,r\}/\min\{t,r\}$.

### C. Numerical Results and Discussions

In Figs. 3, 4 and 5, we compare our CFAs, i.e. equations (15) and (18), with the approximation method of [6] and the nearly-exact $E_b/N_0$ as a function of $C$ that has been obtained via (10). Indeed, equation (10) provides us with the SE $C$ for a given SNR $\gamma$; then, one can easily obtain the SNR $\gamma = f^{-1}(C)$ for a given SE $C$ by using (10) in conjunction with a simple line search algorithm where we set the target $C$ to differ by less than $10^{-8}$ from the actual $C$. Using this approach, we have obtained $f^{-1}(C)$ for $C = 10^{-2}$ to 40 bit/s/Hz with an incremental step of 0.5 bit/s/Hz; then, by inserting $f^{-1}(C)$ and $S = C$ in (3), we have plotted the nearly-exact $E_b/N_0$ as a function of $C$. Regarding the method of [6], note that the values of $\frac{E_b}{N_0}_{\min}$ and $S_0$ are given in equations (213) and (215) of [6], respectively, such that $\frac{E_b}{N_0}_{\min} = \ln(2)/r$ and $S_0 = \frac{2tr}{t+r}$ when equal power allocation is assumed and the MIMO Rayleigh fading channel is unknown at the transmitter.

In Figs. 3 and 4, we first compare the nearly-exact $E_b/N_0$ against the $E_b/N_0$ obtained via our CFAs and the approximation method of [6], respectively. We depict $\Delta_{E_b/N_0}$ (dB), i.e. the approximation error between the nearly-exact $E_b/N_0$ and approximated $E_b/N_0$ values, as a function of $C$ and $\overline{\beta}$. We used incremental steps of 0.25 and 0.5 for $\overline{\beta} \in [1, 10]$ and $\overline{\beta} \in (10, 20]$, respectively. On each figure, the white-colored area represents the area where $\Delta_{E_b/N_0} \leq 0.1$ (dB), whereas the colored area represents the area where $\Delta_{E_b/N_0} > 0.1$ (dB). The color (from yellow to red) indicates the intensity of the error. Figure 3 clearly indicates the great accuracy of our CFAs for a wide range of $C$ and $\overline{\beta}$ values since this graph is mainly white. The maximum approximation error for our method is $\Delta_{E_b/N_0} = 0.16$ dB. In contrast, the results in Fig. 4 show that the approximation method of [6] is mainly accurate for low $C$ values and that the approximation error increases with $C$ to up to $\Delta_{E_b/N_0} = 40$ dB. In order to put things into perspective and help the reader to understand the scale of the approximation error, we plot in Fig. 5 the curves of the nearly-exact $E_b/N_0$, the $E_b/N_0$ obtained via our CFAs and the approximation method of [6] for some specific $\overline{\beta}$ values, i.e. from left to right $\overline{\beta} = \{1.6, 1, 19.5, 1.5, 20, 2\}$ which corresponds to the following antenna configurations $r \times t = \{5\times8, 4\times4, 2\times39, 2\times3, 1\times20, 1\times2\}$, respectively. The results clearly demonstrate the tight fitness between the nearly-exact $E_b/N_0$ curves and our CFAs, hence, they graphically confirm the great accuracy of the latter. They also confirm the poor accuracy of the method of [6] for $C \geq 4$ bit/s/Hz.

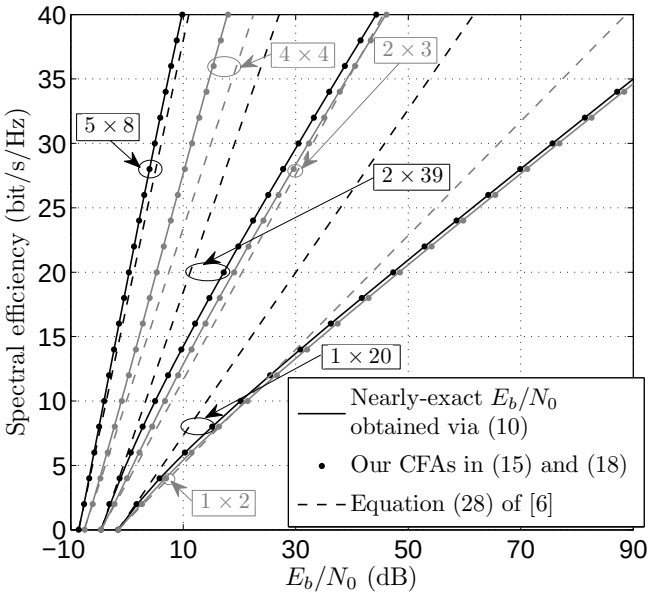


Fig. 5. Comparison of our EE-SE trade-off CFAs in (15) and (18) with the approximation method of [6] and the nearly-exact $E_b/N_0$ obtained via (10) for various $r \times t$ antenna configurations.

## V. Energy Efficiency Gain of MIMO over SISO System

The EE being a ratio between the rate and the power, the EE gain between two systems can either be the result of a system providing a better rate than the other system for a fixed transmit power, or a lower power consumption for a fixed rate, when both systems are affected by the same level of noise and occupy the same bandwidth. In other words, the EE gain is either due to an increase of SE or a decrease in consumed power. MIMO is already well-known to be very effective for the former [26], thus as in [4], our analysis is focused on the latter, more precisely on how efficient is MIMO for reducing the consumed power over the Rayleigh fading channel.

### A. Lower and Upper Limits for the Energy Efficiency Gain

In order to evaluate how MIMO compare with SISO system in terms of EE, we define the EE gain of MIMO over SISO as follows

$$G_{\text{EE}} \triangleq \frac{E_{b,\text{SISO}}}{E_{b,\text{MIMO}}}, \tag{30}$$

which simplifies according to (3) as $G_{\text{EE,Th}} = f^{-1}_{\text{SISO}}(C)/f^{-1}_{\text{MIMO}}(C)$ when assuming a theoretical PCM and where $f^{-1}_{\text{MIMO}}(C)$ is approximated in (15) and (18). In addition, $f^{-1}_{\text{SISO}}(C)$ can be numerically obtained by using the closed-form expression of the MISO SE in (2.47) of [26] for $t = 1$. The latter expression has no generic explicit formulation for $f^{-1}_{\text{MISO}}(C)$, however, we have derived in Section C of the Appendix (see equations (46) and (51)) CFAs of $f^{-1}_{\text{MISO}}(C)$ in the low and high-SE regimes, i.e. when $C \ll 1$ and $C \gg m$, respectively. Moreover, our CFA for MIMO in (15) can also be simplified in the low and high-SE regimes as it is explained in Section D of the Appendix (see equations (56) and (59)). Consequently, the theoretical EE gain of MIMO against SISO system in the low and high-SE regimes, i.e. $G^0_{\text{EE,Th}}$ and $G^\infty_{\text{EE,Th}}$, respectively, can be approximated as

$$\begin{aligned} G^0_{\text{EE,Th}} &\approx r \\ G^\infty_{\text{EE,Th}} &\approx \left(\overline{\beta}-1\right)^{(1-\overline{\beta})} \overline{\beta}^{\left(\overline{\beta}-\frac{1-\zeta}{2}\right)} e^{(\phi-1)} 2^{C\left(1-\frac{1}{m}\right)}, \end{aligned} \tag{31}$$

where $\phi = 0.57721...$ is the Euler-Mascheroni constant [32]. Notice that $G^\infty_{\text{EE,Th}} \approx e^{(\phi-1)} 2^{C\left(1-\frac{1}{m}\right)}$ in the symmetric antenna configuration. Assuming that both SISO and MIMO systems are affected by the same level of noise then $G_{\text{EE,Th}}$ is equivalent to $G_{\text{EE,Th}} = P_{\text{SISO}}/P_{\text{MIMO}}$, where $P_{\text{SISO}}$ and $P_{\text{MIMO}}$ are the respective SISO and MIMO transmit powers. Then we can express the practical EE gain of MIMO against SISO system by inserting (7) into (30) and using the previous definition of $G_{\text{EE,Th}}$ such that

$$G_{\text{EE,Pr}} = \frac{\Delta_P P_{\text{SISO}} + P_0 + P_1}{\Delta_P \frac{P_{\text{SISO}}}{G_{\text{EE,Th}}} + tP_0 + P_1} = \frac{\psi + 1 + \frac{P_1}{P_0}}{\frac{\psi}{G_{\text{EE,Th}}} + t + \frac{P_1}{P_0}}, \tag{32}$$

where $\psi$ is the power ratio given by $\psi \triangleq \frac{\Delta_P P_{\text{SISO}}}{P_0}$. Inserting (31) into (32), we can easily obtained the practical EE gain of MIMO against SISO system in the low and high-SE regimes, i.e. $G^0_{\text{EE,Pr}}$ and $G^\infty_{\text{EE,Pr}}$, respectively. It can be remarked in (31) that $G^\infty_{\text{EE,Th}} \gg 1$ as long as $m > 1$ and, hence, $G^\infty_{\text{EE,Pr}}$ can be formulated as

$$\begin{aligned} G^\infty_{\text{EE,Pr}} \approx \left(\psi + 1 + \frac{P_1}{P_0}\right) \Bigg( &[1 - \text{sgn}(m-1)]\psi(n-1)^{n-1} \\ &\times n^{-\left(n-\frac{1-\zeta}{2}\right)} e^{(1-\phi)} + t + \frac{P_1}{P_0} \Bigg)^{-1}. \end{aligned} \tag{33}$$

Comparing the second equation of (31) with (33) unveils an interesting paradox in the high SE regime; the second equation of (31) clearly indicates that the theoretical EE gain increases with the SE (exponentially) as well as the number of antennas. Whereas equation (33) shows that the EE gain decreases with the number of transmit antennas when $m > 1$ and a double linear PCM is considered and, consequently, that $t = 2$ is the most energy efficient number of transmit antennas in the high-SE regime when $r > 1$. Also, (33) reveals that if $\psi < 1$ then MIMO cannot be more EE than SISO, when $m > 1$.

### B. Numerical Results and Discussions

Figures 6 and 8 depict the theoretical EE gain as a function of the SE for various antenna configurations and the number of antenna elements $n_{\text{ant}} = t = r$ for various $C$ values, respectively. The results in Fig. 6 confirm that the theoretical EE gain increases exponentially (linearly in log-scale) with the SE when receive diversity is available, i.e. $r > 1$. In the case of $r = 1$, i.e. $m = 1$, $G_{\text{EE}}$ is then independent of $C$ and the EE gain is bounded by $2e^{(\phi-1)} \simeq 1.31$ for $t = 2$ according to (31). Moreover, Fig. 8 confirms that the theoretical EE gain also increases with the number of antennas. This behavior is directly related to the behavior of the term $(1 - \frac{1}{m})$ in (31), which increases as $m = n_{\text{ant}}$ increases. Furthermore, results in both figures clearly show that our limits for the theoretical EE gain at low and high SE in (31) are accurate; on the one hand, the EE gain at $C = 0$ in Fig. 6 is $G_{\text{EE}} = \{1, 2, 3, 3\}$ for $r \times t = \{1 \times 2, 2 \times 2, 3 \times 2, 3 \times 3\}$, respectively, which is consistent with $G^0_{\text{EE,Th}} \approx r$. Whereas the curve of $G^0_{\text{EE,Th}}$ tightly matches the curve of $G_{\text{EE}}$ for $C = 10^{-2}$ bit/s/Hz in Fig. 8. On the other hand, the curves of $G_{\text{EE}}$ and $G^\infty_{\text{EE,Th}}$ tightly fit each others for large values of $C$ in Fig. 6 and $G^\infty_{\text{EE,Th}}$ tightly fits $G_{\text{EE}}$ for $C = 40$ bit/s/Hz in Fig. 8 when $n_{\text{ant}} \leq 5$. Note that $G^\infty_{\text{EE,Th}}$ in (31) has been derived by assuming that $C \gg m = n_{\text{ant}}$, however, this assumption weakens as $n_{\text{ant}} > 5$ and a gap between $G^\infty_{\text{EE,Th}}$ and $G_{\text{EE}}$ appears.

In Figs. 7 and 9, the practical EE gain as a function of the SE and number of antenna elements, respectively, are plotted for different types of BS. The results for Pico and Femto BSs being very similar, the latter has been omitted. We have used the following values for the parameters $\{P_{\max} = 80; \Delta_P = 7.25; P_0 = 244; P_1 = 225\}$, $\{6.31; 3.14; 35; 34\}$ and $\{0.25; 4.4; 6.1; 2.6\}$ for macro, micro and pico BSs, respectively, which have been extrapolated from the values given in Section 4 of [13]. In the SISO case, (10) provides the SE $C$ for a given SNR $\gamma$ and $f^{-1}_{\text{SISO}}(C)$ can be easily obtained by using the same method described in Section IV-C for $C = 10^{-2}$ to $40$ bit/s/Hz with an incremental step of 0.5 bit/s/Hz. We have then assumed a fixed transmit power $P_{\max}$ for each $C$ value and have computed the noise $N_{\text{SISO}}(\text{dB}) =$

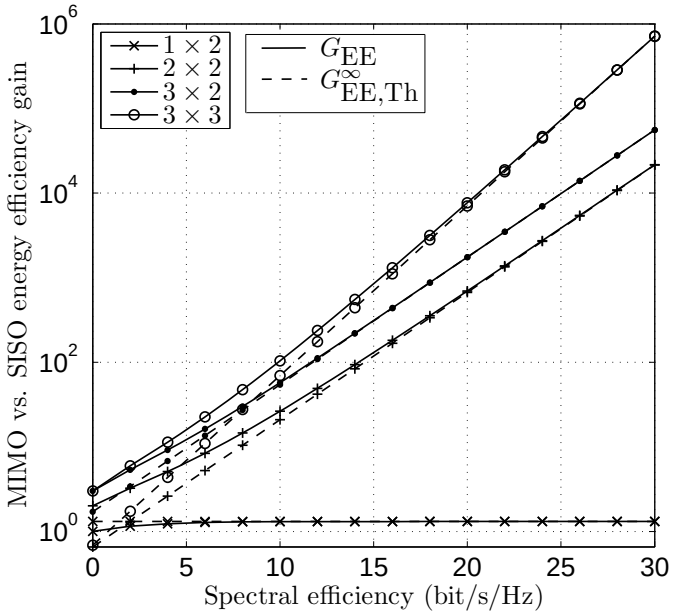


Fig. 6. MIMO vs. SISO EE gain against the SE when considering the theoretical PCM.

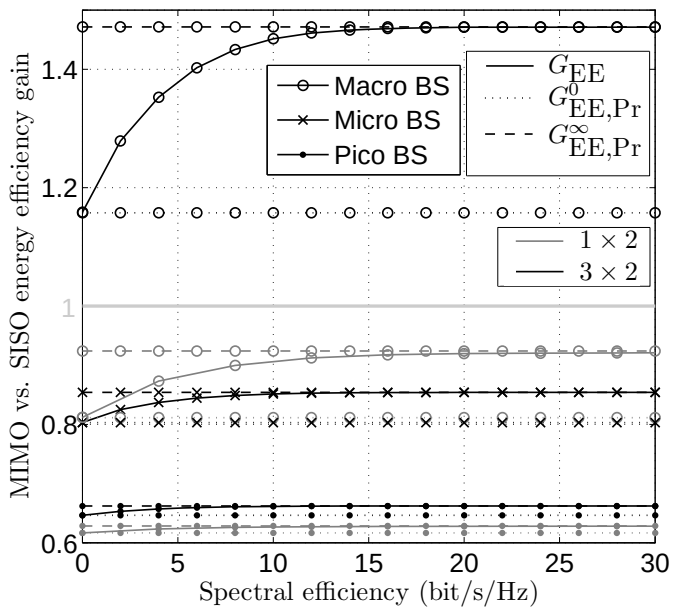


Fig. 7. MIMO vs. SISO EE gain against the SE for different types of BS when considering the double linear PCM of (6).

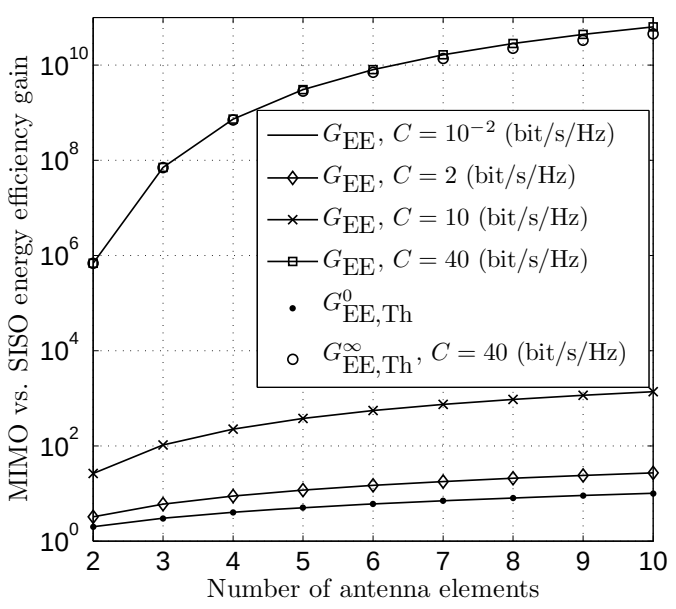


Fig. 8. MIMO vs. SISO EE gain against the number of antenna elements $n_{\text{ant}} = t = r$ when considering the theoretical PCM.

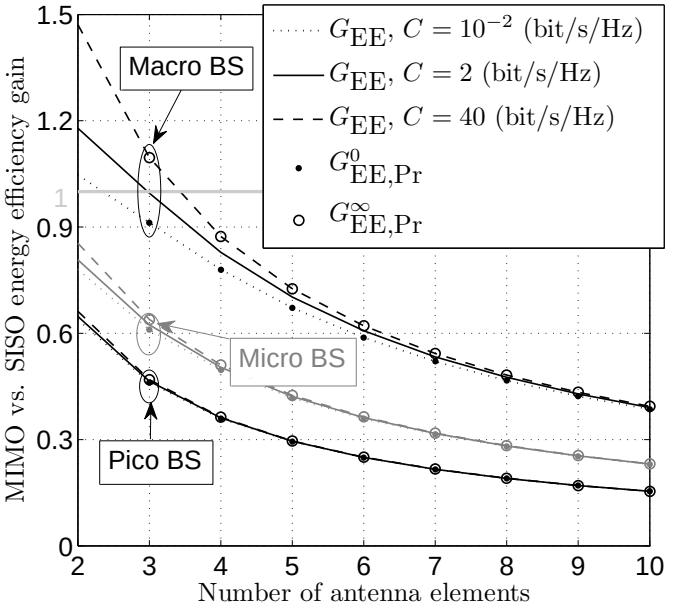


Fig. 9. MIMO vs. SISO EE gain against the number of antennas $n_{\text{ant}} = t = r$ for different types of BS when considering the double linear PCM of (6).

$P_{\text{SISO}}(\text{dB}) - f^{-1}_{\text{SISO}}(C)(\text{dB})$. In MIMO case, we have used our closed-form in (15) for obtaining $f^{-1}_{\text{MIMO}}(C) \approx \widetilde{f}^{-1}(C)$ and then computed $P_{\text{MIMO}}(\text{dB}) = f^{-1}_{\text{MIMO}}(C)(\text{dB}) + N_{\text{SISO}}(\text{dB})$. In other words, we have obtained the transmit power $P$ that is required by MIMO for achieving the same SE as SISO for a fixed noise power. This transmit power is always lower for MIMO than for SISO but it is not necessarily the case for the total consumed power $P_{\Sigma}$, as it is hinted by the results of Figs. 7 and 9. Indeed, in comparison with the results of Figs. 6 and 8, only a very limited EE gain, i.e. no more than 1.46, can be achieved for the macro BS scenario when $n_{\text{ant}} = 2$. In most of the other depicted cases, SISO is more EE than MIMO. The results also indicate that $G_{\text{EE}}$ increases with $C$ but decreases with the number of transmit antennas when $m > 1$, which was indicated by our analytical result in (33). Thus, the most desirable number of transmit antennas in terms of EE is two, as it is confirmed by Fig. 9. As in the theoretical case, our limits for the practical EE gain at low and high SE, i.e. $G^{0}_{\text{EE,Pr}}$ and $G^{\infty}_{\text{EE,Pr}}$, tightly match $G_{\text{EE}}$ for $C = 10^{-2}$ and 40 bit/s/Hz , respectively. Moreover, they clearly act as lower and upper bounds for $G_{\text{EE}}$ such that the maximum practical EE gain is given by (33), where the ratio $\psi$ can be a simple criteria for

assessing whether or not to use MIMO for EE purpose. For instance, we obtain that $\psi \simeq 2.38, 0.57$ and 0.18 for macro, micro and pico BSs, respectively, by computing $\psi$ for the three types of BS of Figs. 7 and 9. This confirms that if $\psi < 1$ then SISO is more EE than MIMO.

## VI. Conclusion

In this paper, an accurate closed-form approximation of the EE-SE trade-off over the MIMO Rayleigh fading channel has been derived by considering different types of PCM. We have first introduced our new approach for obtaining an explicit formulation of the EE-SE trade-off and have provided a formal proof of the derivation for the symmetric antenna case. Next, we have extended this approach to various other antenna settings by means of an heuristic curve fitting method. The accuracy of our approximation has been shown experimentally for numerous antenna configurations and a wider range of SE values than the previous best-accurate approximation in [6]. Our EE-SE trade-off expression has then been utilized for evaluating analytically the EE gain limits of MIMO over SISO system in the low and high-SE regimes for either the theoretical or a double linear PCM. In the high-SE regime, the theoretical EE gain increases with the SE as well as the number of antennas, whereas the practical EE gain decreases with the number of transmit antennas. Simulation results have confirmed our analytical results and have shown the large discrepancy between the theoretical and practical MIMO/SISO EE gains; in theory, MIMO has a great potential for EE improvement over the Rayleigh fading channel; in practice, when a realistic PCM is considered, a MIMO system with two transmit antennas is not necessarily more EE than a SISO system and utilizing more than two transmit antennas is likely to be energy inefficient, which is consistent with the findings in [4] for sensor networks. In the future, we would like to use our CFA based approach for deriving the EE-SE trade-off of cooperative MIMO system.

## Acknowledgment

The first author wish to thank his beloved wife for her support and helpful comments in improving the readability of this paper.

## Appendix

### A. Derivation Insights: from equation (12) to (14)

Let us re-express $q_0(\gamma)$ in (13) as follows

$$\begin{aligned} q_0(\gamma) &= \frac{-1-u(\gamma)+v(\gamma)}{2\sqrt{\gamma}} \\ &= \frac{[-1-u(\gamma)+v(\gamma)][1+u(\gamma)+v(\gamma)]}{2\sqrt{\gamma}[1+u(\gamma)+v(\gamma)]} \\ &= \frac{4\beta\gamma}{2\sqrt{\gamma}[2-1+u(\gamma)+v(\gamma)]} = \frac{4\beta\gamma}{2\sqrt{\gamma}[2+2\sqrt{\gamma}r_0(\gamma)]} \\ &= \frac{\beta\sqrt{\gamma}}{1+\sqrt{\gamma}r_0(\gamma)} \end{aligned} \tag{34}$$

and similarly,

$$r_0(\gamma) = \frac{\sqrt{\gamma}}{1+\sqrt{\gamma}q_0(\gamma)}. \tag{35}$$

It then implies that

$$\begin{aligned} \sqrt{\gamma}q_0(\gamma)r_0(\gamma) &= \beta\sqrt{\gamma} - q_0(\gamma) \\ &= \sqrt{\gamma} - r_0(\gamma) \end{aligned}. \tag{36}$$

Adding up the two equalities in (36), we simply obtain that

$$q_0(\gamma)r_0(\gamma) = \frac{1}{2}\left(\beta + 1 - \frac{q_0(\gamma)+r_0(\gamma)}{\sqrt{\gamma}}\right). \tag{37}$$

Inserting equation (37) into (12), the latter can be re-expressed as follows

$$\begin{aligned} \widetilde{f}(\gamma) &= -\frac{t}{\ln(2)}\left[\frac{1}{2}\left\{1 - \frac{r_0(\gamma)}{\sqrt{\gamma}} + 2\ln\left(\frac{r_0(\gamma)}{\sqrt{\gamma}}\right)\right\}\right. \\ &\quad \left. + \frac{\beta}{2}\left\{1 - \frac{q_0(\gamma)}{\beta\sqrt{\gamma}} + 2\ln\left(\frac{q_0(\gamma)}{\beta\sqrt{\gamma}}\right)\right\}\right]. \end{aligned} \tag{38}$$

Substituting $q_0(\gamma)$ and $r_0(\gamma)$ by (34) and (35), respectively, equation (38) is transformed as

$$\begin{aligned} \widetilde{f}(\gamma) = -\frac{1}{\ln(2)}\left[\frac{t}{2}\left\{1 - \frac{2}{2+2\sqrt{\gamma}q_0(\gamma)} + 2\ln\left(\frac{2}{2+2\sqrt{\gamma}q_0(\gamma)}\right)\right\}\right. \\ \left. + \frac{r}{2}\left\{1 - \frac{2}{2+2\sqrt{\gamma}r_0(\gamma)} + 2\ln\left(\frac{2}{2+2\sqrt{\gamma}r_0(\gamma)}\right)\right\}\right], \end{aligned} \tag{39}$$

which is finally equivalent to (14) when replacing $q_0(\gamma)$ and $r_0(\gamma)$ by $q_0(\gamma) \triangleq (\overline{q}_0(\gamma)-1)/2\sqrt{\gamma}$ and $r_0(\gamma) \triangleq (\overline{r}_0(\gamma)-1)/2\sqrt{\gamma}$, respectively.

### B. Derivation Insights: equation (25)

The expression $S_r - S_t$ can be formulated as $S_r - S_t = r(\ln[1+\overline{r}_0(\gamma)] - \ln(2)) - t(\ln[1+\overline{q}_0(\gamma)] - \ln(2)) + \underbrace{r\left(-1/2 + [1+\overline{r}_0(\gamma)]^{-1}\right) - t\left(-1/2 + [1+\overline{q}_0(\gamma)]^{-1}\right)}_{A}$ according to the definition of $S_r$ and $S_t$ in (14). Subtracting the second equation of (36) from the first, we obtain that

$$\beta\sqrt{\gamma} - q_0(\gamma) - (\sqrt{\gamma} - r_0(\gamma)) = 0, \tag{40}$$

which can be further transformed as

$$r\left(1 - \frac{q_0(\gamma)}{\beta\sqrt{\gamma}}\right) - t\left(1 - \frac{r_0(\gamma)}{\sqrt{\gamma}}\right) = 0. \tag{41}$$

Substituting $q_0(\gamma)$ and $r_0(\gamma)$ by (34) and (35), respectively, and replacing $q_0(\gamma)$ and $r_0(\gamma)$ by $q_0(\gamma) \triangleq (\overline{q}_0(\gamma)-1)/2\sqrt{\gamma}$ and $r_0(\gamma) \triangleq (\overline{r}_0(\gamma)-1)/2\sqrt{\gamma}$, we finally obtain that

$$r\left(1 - 2[1+\overline{r}_0(\gamma)]^{-1}\right) - t\left(1 - 2[1+\overline{q}_0(\gamma)]^{-1}\right) = -2A = 0. \tag{42}$$

Thus, $A$ is equal to zero and $S_r - S_t$ simplifies as $S_r - S_t = \ln(2^t[1+\overline{r}_0(\gamma)]^r) - \ln(2^r[1+\overline{q}_0(\gamma)]^t)$.

### C. Limits of the EE-SE trade-off for MISO channel in the Low and High-SE regimes

The MISO capacity can be expressed as $C = \widehat{f}(\gamma) = \widehat{C}_{t-1}(t/\gamma)/\Gamma(t)$ [26], [29], where $\widehat{C}_i(x)$ is given in (11) and $\Gamma(x) \triangleq (x-1)!$ is the Gamma function. According to (11), the function $\widehat{f}(\gamma)$ can be formulated as $C =$

$$\widehat{f}(\gamma) = \underbrace{\left(\sum_{i=0}^{t-1} \frac{(-z)^i}{\Gamma(i+1)}\right)}_{A(z)} \frac{e^z E_1(z)}{\ln(2)} + \underbrace{\sum_{i=0}^{t-2} \frac{(-z)^i}{\ln(2)} \sum_{j=i}^{t-2} \frac{\Gamma(j-i+1)}{\Gamma(j+2)}}_{B(z)}, \tag{43}$$

where $z \triangleq t/\gamma$.

*1) Low-SE regime:* The function $E_1(x)$ can be approximated as $E_1(x) \overset{\infty}{\approx} \frac{e^{-x}}{x}\left(\sum_{u=0}^{U-1} \frac{\Gamma(u+1)}{(-x)^u}\right)$ with $U \gg 1$, i.e. $U \geq t$, when $x$ approaches infinity [33]. Thus, in the case that $\gamma \to 0$, i.e. $z \to \infty$, $A(z)e^z E_1(z)$ becomes equivalent to

$$\begin{aligned} A(z)e^z E_1(z) \overset{\gamma \to 0}{\sim} & \frac{t}{z} - \sum_{i=0}^{U-2} (-z)^i \sum_{j=i}^{t-2} \frac{\Gamma(j-i+1)}{\Gamma(j+2)} \\ & - \frac{1}{z^2} \sum_{i=0}^{U-2} (-z)^{-i} \sum_{j=i}^{t-2} \frac{\Gamma(j+2)}{\Gamma(j-i+1)}, \end{aligned} \tag{44}$$

and $C$ in (43) can be re-expressed as

$$C \overset{0}{\sim} \frac{1}{z\ln(2)} \left( \sum_{i=0}^{U-1} (-z)^{-i} \sum_{j=i}^{\min(i+t-1, U-1)} \frac{\Gamma(j+1)}{\Gamma(j+1-i)} \right), \tag{45}$$

which further simplifies as $C \overset{0}{\sim} \frac{t}{z\ln(2)} = \frac{\gamma}{\ln(2)}$ by considering only the first order approximation. Consequently, we obtain that

$$\gamma = \widehat{f}^{-1}(C) \overset{0}{\sim} C\ln(2) \tag{46}$$

in the low-SE regime.

*2) High-SE regime:* The first order approximations of $e^x, E_1(x), A(x)$ and $B(x)$ are given by

$$\begin{aligned} & e^x \overset{0}{\sim} 1 + x \\ & E_1(x) = -\phi - \ln(x) + \sum_{i=1}^{\infty} \frac{(-1)^{i+1} x^i}{i\, i!} \overset{0}{\sim} -\phi - \ln(x) + x \\ & A(x) \overset{0}{\sim} 1 - x \\ & B(x) \overset{0}{\sim} \frac{1}{\ln(2)} \left( \sum_{i=1}^{t-1} \frac{1}{i} + x \sum_{i=1}^{t-2} \frac{\Gamma(i)}{\Gamma(i+2)} \right) \end{aligned}, \tag{47}$$

respectively, where $\phi = 0.57721...$ is the Euler-Mascheroni constant [32]. In the case that $\gamma \to \infty$, i.e. $z \to 0$, $C$ can be approximated by inserting the function approximations of (47) in (43), as follows

$$C \overset{\gamma \to \infty}{\sim} \frac{1}{\ln(2)} \underbrace{\left(-\phi + \sum_{i=1}^{t-1} \frac{1}{i}\right)}_{a(t)} + \frac{z}{\ln(2)} \underbrace{\left(1 - \sum_{i=1}^{t-2} \frac{\Gamma(i)}{\Gamma(i+2)}\right)}_{b(t)} - \log_2(z). \tag{48}$$

The approximation in (48) can be re-expressed as $C\ln(2) - a(t) \overset{\infty}{\approx} zb(t) - \ln(z)$, which in turn is equivalent to

$$-b(t)2^{-C} e^{a(t)} \overset{\infty}{\approx} -zb(t)e^{-zb(t)}, \tag{49}$$

since $b(t) \geq 0$. Moreover $b(t) \in [0,1]$ and $z \ll 1$, which implies that $-zb(t)e^{-zb(t)} \in [-e^{-1}, 0]$. Consequently, $-b(t)2^{-C}e^{a(t)}$ also belongs to $[-e^{-1}, 0] \subset \mathcal{D}_{W_0}$ and, hence, (49) can be reformulated as

$$\widehat{f}^{-1}(C) = \gamma \overset{\infty}{\approx} \frac{-tb(t)}{W_0\left(-b(t)e^{a(t)}2^{-C}\right)}. \tag{50}$$

Moreover, we know that $C$ grows linearly with $\gamma$ (dB) when $\gamma \gg t$, i.e. $z \to 0$. It implies that $C \gg 1$ and $2^{-C} \to 0$ when $z \to 0$ and, consequently, (50) can be simplified as

$$\widehat{f}^{-1}(C) \overset{\infty}{\approx} te^{-a(t)}2^C, \tag{51}$$

since $W_0(x) \overset{0}{\sim} x$. Finally, it can be noticed that (51) further simplifies as $\widehat{f}^{-1}(C) \overset{\infty}{\approx} 2^C$ when $t$ approaches infinity since $a(t) \overset{\infty}{\approx} \ln(t-1)$ and $t/(t-1) \overset{\infty}{\approx} 1$.

### D. Limits of the EE-SE trade-off for MIMO channel in the Low and High-SE regimes

By using our CFA of the EE-SE trade-off for the MIMO channel, we can derive simplified expressions of this trade-off for both the low and high-SE regimes.

*1) Low-SE regime:* In the case that $x \ll 1$, the function $h(x)$ in (17) can be approximated as

$$h(x) \overset{0}{\sim} \frac{\zeta\eta_0\eta_1 \ln(2)}{2m} \left( \frac{x}{\eta(\overline{\beta}) + \log_2(\eta_0)} \right)^2 \tag{52}$$

by applying the following approximations of usual functions $\cosh(x) \overset{0}{\sim} 1 + x^2/2$, $\ln(1+x) \overset{0}{\sim} x$ and $e^x \overset{0}{\sim} 1 + x$. Consequently, the first order approximation of $x \pm h(x) \overset{0}{\sim} x$ and, hence, $g_t(x) \overset{0}{\sim} -2^{-\left(\frac{x}{2t}+1\right)}e^{-\frac{1}{2}}$ as well as $g_r(x) \overset{0}{\sim} -2^{-\left(\frac{x}{2r}+1\right)}e^{-\frac{1}{2}}$ in (16). The function $g_t(x)$ can further be simplified as follows

$$\begin{aligned} g_t(x) & \overset{0}{\sim} -\frac{1}{2} e^{-\left(\frac{x\ln(2)}{t}\right)} e^{-\frac{1}{2}\left(1 - \frac{x\ln(2)}{t}\right)} \\ & \overset{0}{\sim} -\frac{1}{2}\left(1 - \frac{x\ln(2)}{t}\right) e^{-\frac{1}{2}\left(1 - \frac{x\ln(2)}{t}\right)} \end{aligned} \tag{53}$$

by rearranging the terms of $g_t(x)$ and then applying $e^x \overset{0}{\sim} 1 + x$, which in turn leads to

$$W_0(g_t(C)) \overset{0}{\sim} -\frac{1}{2}\left(1 - \frac{C\ln(2)}{t}\right) \tag{54}$$

in (15), when $C \ll 1$. Similarly, $W_0(g_r(C)) \overset{0}{\sim} -\frac{1}{2}\left(1 - \frac{C\ln(2)}{r}\right)$. Inserting the approximations for $W_0(g_t(C))$ and $W_0(g_r(C))$ in (15), we obtain that

$$\begin{aligned} \widetilde{f}^{-1}(C) & \overset{0}{\sim} \frac{-2r(t - C\ln(2)) - 2t(r - C\ln(2)) + 4rt}{2(1+\beta)(t - C\ln(2))(r - C\ln(2))} \\ & \overset{0}{\sim} \frac{2C\ln(2)(t+r)}{2(1+\beta)rt}, \end{aligned} \tag{55}$$

which finally simplifies as

$$\widetilde{f}^{-1}(C) \overset{0}{\sim} = C\ln(2)/r, \tag{56}$$

when $C \ll 1$. This result is consistent with (213) of [6].

*2) High-SE regime:* In the case that $x \gg 1$, the function $h(x)$ in (17) can be approximated as

$$h(x) \overset{\infty}{\approx} \zeta \left\{ \frac{\eta_1 x}{\eta(\overline{\beta}) + \log_2(\eta_0)} - m[\eta_1 - \log_2(\eta_0)] \right\}, \quad (57)$$

since $\cosh(x) \overset{\infty}{\approx} e^x/2$. In the case that $\eta_1 = \eta(\overline{\beta}) + \log_2(\eta_0)$, i.e. when $\overline{\beta} \in [2, +\infty) \cup \{4/3, 3/2, 8/5, 5/3, 7/4, 9/5\}$, then $h(x)$ in (17) simplifies as $h(x) \overset{\infty}{\approx} \zeta[x - m\eta(\overline{\beta})]$. Moreover, $x \pm h(x) \overset{\infty}{\approx} x = 2x\delta(\zeta \pm 1) - \zeta m\eta(\overline{\beta})$, where $\delta(x) = 1$ if $x = 0$ and 0 else. In other words, either $g_r(x)$ or $g_t(x)$ is independent of $x$ when $\beta > 1$ or $\beta < 1$, respectively. Let us first assume that $\beta > 1$, i.e. $\zeta = 1$, $r > t$, $m = t$ and $\overline{\beta} = \beta$, then

$$\begin{aligned} g_t(x) &\overset{\infty}{\approx} -\frac{1}{2} e^{-\frac{1}{2}\left(1 + \left[\frac{2x}{t} - \eta(\overline{\beta})\right] \ln(2)\right)} = -\frac{e^{-1}}{2} \left(\frac{\overline{\beta} - 1}{\overline{\beta}}\right)^{-\overline{\beta}} 2^{-\frac{x}{t}} \\ g_r(x) &\overset{\infty}{\approx} -\frac{1}{2} e^{-\frac{1}{2}\left(1 + \frac{\eta(\overline{\beta}) \ln(2)}{\beta}\right)} = -\frac{\overline{\beta} - 1}{2\overline{\beta}} e^{-\frac{\overline{\beta} - 1}{2\overline{\beta}}} \end{aligned}. \quad (58)$$

On the one hand, $g_t(x) \overset{\infty}{\approx} 0$ since $e^{-(x/a+b)} \overset{\infty}{\approx} 0$ and, thus, $W_0(g_t(C)) \overset{\infty}{\approx} g_t(C)$ since $W_0(x) \overset{0}{\sim} x$. On the other hand, $W_0(g_r(C)) \overset{\infty}{\approx} -\frac{\overline{\beta}-1}{2\overline{\beta}}$. Likewise, in the case that $\beta < 1$, $W_0(g_t(C)) \overset{\infty}{\approx} -\frac{\overline{\beta}-1}{2\overline{\beta}}$ and $W_0(g_r(C)) \overset{\infty}{\approx} g_r(C) \overset{\infty}{\approx} -\frac{e^{-1}}{2}\left(\frac{\overline{\beta}-1}{\overline{\beta}}\right)^{-\overline{\beta}} 2^{-\frac{x}{r}}$. Notice that the approximations $W_0(g_t(C)) \overset{\infty}{\approx} g_t(C)$ and $W_0(g_r(C)) \overset{\infty}{\approx} g_r(C)$ require not only that $C \gg 1$ but $C \gg m$. Inserting the approximations for $W_0(g_t(C))$ and $W_0(g_r(C))$ in (15), we finally obtain that

$$\widetilde{f}^{-1}(C) \overset{\infty}{\approx} \left(\overline{\beta} - 1\right)^{\overline{\beta}-1} \overline{\beta}^{-\left(\overline{\beta} - \frac{1-\zeta}{2}\right)} e^1 2^{\frac{C}{m}} \quad (59)$$

when $C \gg m$, for any $\overline{\beta} \in [2, +\infty) \cup \{4/3, 3/2, 8/5, 5/3, 7/4, 9/5\}$, which further simplifies as

$$\widetilde{f}^{-1}(C) \overset{\infty}{\approx} e^1 2^{\frac{C}{m}} \quad (60)$$

for $\beta = 1$, i.e. when $t = r$.

## REFERENCES


[1] K. Lahiri, A. Raghunathan, S. Dey, and D. Panigrahi, "Battery-driven System Design: A New Frontier in Low Power Design," in *Proc. Intl. Conf. on VLSI Design*, Bangalore, India, Jan. 2002, pp. 261–267.

[2] H. M. Kwon and T. G. Birdsall, "Channel Capacity in Bits per Joule," *IEEE J. Ocean. Eng.*, vol. OE-11, no. 1, pp. 97–99, Jan. 1986.

[3] C. Bae and W. E. Stark, "Energy and Bandwidth Efficiency in Wireless Networks," in *Proc. IEEE ICCCAS*, Guilin, China, Jun. 2006.

[4] S. Cui, A. J. Goldsmith, and A. Bahai, "Energy-Efficiency of MIMO and Cooperative MIMO Techniques in Sensor Networks," *IEEE J. Sel. Areas Commun.*, vol. 22, no. 6, pp. 1089–1098, Aug. 2004.

[5] 3GPP TSG-SA#50 SP-1008883GPP, 3GPP Work Item Description, "Study on System Enhancements for Energy Efficiency," 3GPP TSG-SA, Istanbul, Turkey, Tech. Rep., Dec. 2010, agreed Work Item 500037 (Release 11).

[6] S. Verdu, "Spectral Efficiency in the Wideband Regime," *IEEE Trans. Inf. Theory*, vol. 48, no. 6, pp. 1319–1343, Jun. 2002.

[7] A. Lozano, A. M. Tulino, and S. Verdu, "Multiple-antenna Capacity in the Low-power Regime," *IEEE Trans. Inf. Theory*, vol. 49, no. 10, pp. 2527–2544, Oct. 2003.

[8] O. Oyman and A. J. Paulraj, "Spectral Efficiency of Relay Networks in the Power Limited Regime," in *Proc. 42th Annual Allerton Conf. on Communication, Control and Computing*, Allerton, USA, Sep. 2004.

[9] V. Rodoplu and T. H. Meng, "Bits-per-Joule Capacity of Energy-limited Wireless Networks," *IEEE Trans. Wireless Commun.*, vol. 6, no. 3, pp. 857–865, Mar. 2007.

[10] J. Gómez-Vilardebó, A. I. Pérez-Neira, and M. Nájar, "Energy Efficient Communications over the AWGN Relay Channel," *IEEE Trans. Wireless Commun.*, vol. 9, no. 1, pp. 32–37, Jan. 2010.

[11] O. Arnold, F. Richter, G. Fettweis, and O. Blume, "Power Consumption Modeling of Different Base Station Types in Heterogeneous Cellular Networks," in *Proc. ICT Future Network & Mobile Summit*, Florence, Italy, Jun. 2010.

[12] A. Fehske, P. Marsch, and G. Fettweis, "Bit per Joule Efficiency of Cooperating Base Stations in Cellular Networks," in *Proc. IEEE Globecom Workshops (GC Wkshps)*, Miami, USA, Dec. 2010.

[13] G. Auer et al., "D2.3: Energy Efficiency Analysis of the Reference Systems, Areas of Improvements and Target Breakdown," INFSO-ICT-247733 EARTH (Energy Aware Radio and NeTwork TecHnologies), Tech. Rep., Nov. 2010.

[14] G. Caire, G. Taricco, and E. Biglieri, "Suboptimality of TDMA in the Low-power Regime," *IEEE Trans. Inf. Theory*, vol. 50, no. 4, pp. 608–620, Apr. 2004.

[15] Y. Yao, X. Cai, and G. B. Giannakis, "On Energy Efficiency and Optimum Resource Allocation of Relay Transmissions in the Low-power Regime," *IEEE Trans. Wireless Commun.*, vol. 4, no. 6, pp. 2917–2927, Nov. 2005.

[16] O. Somekh, B. M. Zaidel, and S. Shamai, "Sum Rate Characterization of Joint Multiple Cell-site Processing," *IEEE Trans. Inf. Theory*, vol. 53, no. 12, pp. 4473–4497, Dec. 2007.

[17] O. Simeone, O. Somekh, Y. Bar-Ness, and U. Spagnolini, "Throughput of Low-lower Cellular Systems with Collaborative Base Stations and Relaying," *IEEE Trans. Inf. Theory*, vol. 54, no. 1, pp. 459–467, Jan. 2008.

[18] N. C. Beaulieu and F. Rajwani, "Highly Accurate Simple Closed-Form Approximations to Lognormal Sum Distributions and Densities," *IEEE Commun. Lett.*, vol. 8, no. 12, pp. 709–711, Dec. 2004.

[19] D. B. da Costa and M. D. Yacoub, "Average Channel Capacity for Generalized Fading Scenarios," *IEEE Commun. Lett.*, vol. 11, no. 12, pp. 949–951, Dec. 2007.

[20] F. Héliot, O. Onireti, and M. A. Imran, "An Accurate Closed-form Approximation of the Energy Efficiency-Spectral Efficiency Trade-off over the MIMO Rayleigh Fading Channel," in *Proc. IEEE ICC'11, 4-th Internat. Workshop on Green Communications*, Kyoto, Japan, Jun. 2011.

[21] F. Héliot, M. A. Imran, and R. Tafazolli, "On the Energy Efficiency Gain of MIMO Communication under Various Power Consumption Models," in *Proc. ICT Future Network & Mobile Summit*, Warsaw, Poland, Jun. 2011.

[22] C. Shannon, "A Mathematical Theory of Communication," *Bell Syst. Tech. J.*, vol. 27, pp. 379–423, 623–656, July-Oct. 1948.

[23] O. Onireti, F. Héliot, and M. A. Imran, "On the energy efficiency-spectral efficiency trade-off in the uplink of CoMP system," *IEEE Trans. Wireless Commun.*, vol. 11, no. 2, pp. 556–561, Feb. 2012.

[24] J. Xu, L. Qiu, and C. Yu, "Improving energy efficiency through multimode transmission in the downlink MIMO systems," *EURASIP Journal on Wireless Communications and Networking*, 2011, **2011**:200.

[25] I. E. Telatar, "Capacity of Multi-antenna Gaussian Channels," *Europ. Trans. Telecommun. and Related Technol.*, vol. 10, no. 6, pp. 585–596, Nov. 1999.

[26] M. Dohler, "Virtual Antenna Arrays," Ph.D. dissertation, King's College London, University of London, Nov. 2003.

[27] H. Shin and J. Lee, "Closed-form Formulas for Ergodic Capacity of MIMO Rayleigh Fading Channels," in *Proc. IEEE ICC'03*, Anchorage, USA, May 2003, pp. 2996–3000.

[28] M. Kang and M. Alouini, "On the Capacity of MIMO Rician Channels," in *Proc. 40th Annual Allerton Conf. on Communcation, Control and Computing*, 2002, pp. 936–945.

[29] M. Dohler and H. Aghvami, "On the Approximation of MIMO Capacity," *IEEE Trans. Wireless Commun.*, vol. 4, no. 1, pp. 30–34, Jan. 2005.

[30] E. Biglieri and G. Taricco, *Transmission and Reception with Multiple Antennas: Theoretical Foundations*. Now Publishers Inc., 2004.

[31] R. M. Corless, G. H. Gonnet, D. E. G. Hare, D. J. Jeffrey, and D. E. Knuth, "On the LambertW Function," *Adv. Comput. Math.*, vol. 5, pp. 329–359, 1996.

[32] X. Gourdon and P. Sebah, "The Euler constant: $\gamma$." [Online]. Available: http://numbers.computation.free.fr/Constants/Gamma/gamma.html

[33] M. Abramowitz and I. A. Stegun, *Handbook of Mathematical Functions with formulas, Graphs and Mathematical Tables*. New-York, Dover Press, Jun. 1974.

**Fabien Héliot** (S'05-M'07) received the M.Sc. degree in Telecommunications from the Institut Supérieur de l'Electronique et du Numérique (ISEN), Toulon, France, and the Ph.D. degree in Mobile Telecommunications from King's College London, in 2002 and 2006, respectively. He is currently a research fellow at the Centre for Communication Systems Research (CCSR) of the University of Surrey. He has been actively involved in European Commission funded projects such as IST FIREWORKS and IST ROCKET projects. He is currently involved in the ICT EARTH project, which is a leading European project investigating the energy efficiency of mobile communication systems. His main research interests are energy efficiency, cooperative communication, MIMO, and radio resource management.

**Muhammad Ali Imran** (M'03) received his B.Sc. degree in Electrical Engineering from University of Engineering and Technology Lahore, Pakistan, in 1999, and the M.Sc. and Ph.D. degrees from Imperial College London, UK, in 2002 and 2007, respectively. He secured first rank in his BSc and a distinction in his MSc degree along with an award of excellence in recognition of his academic achievements, conferred by the President of Pakistan. He is currently a lecturer in the Centre for Communication Systems Research (CCSR) at the University of Surrey, UK. He has been actively involved in European Commission funded research projects ROCKET and EARTH, Mobile VCE funded project on fundamental capacity limits and EPSRC funded project India UK ATC. He is the principal investigator of EPSRC funded REDUCE project. His main research interests include the analysis and modeling of the physical layer, optimization for the energy efficient wireless communication networks and the evaluation of the fundamental capacity limits of wireless networks.

**Rahim Tafazolli** (SM'09) is a professor and the Director of Centre for Communication Systems Research (CCSR), University of Surrey, United Kingdom. He has been active in research for more than 20 years and has authored and co-authored more than 360 papers in refereed international journals and conferences. Professor Tafazolli is a consultant to many mobile companies, has lectured, chaired, and been invited as keynote speaker to a number of IET and IEEE workshops and conferences. He has been Technical Advisor to many mobile companies, all in the field of mobile communications. He is the Founder and past Chairman of IET International Conference on 3rd Generation Mobile Communications. He is a Fellow of the IET and WWRF (Wireless World Research Forum). He is Chairman of EU Expert Group on Mobile Platform (e-mobility SRA) and Chairman of Post-IP working group in e-mobility, past Chairman of WG3 of WWRF. He is nationally and internationally known in the field of mobile communications.